

Al6063, Pure Aluminium and Brass Casting Solidification using Explicit Scheme

Nitesh Gupta^{1*}, Dinesh Kumar Kasdekar² and Pooja Gupta³

^{*1,2}Department of Mechanical Engineering

³Department of Electronics Engineering

^{*1,2}Madhav Institute of Technology & Science, Gwalior- 474005, India (M.P)

³Lakshmi Narain College of technology & science, Bhopal-462021, India (M.P)

*gupta.nitesh07@gmail.com

Abstract

Finite difference modeling of solidification of pure aluminum, Al 6063 and brass casting in green sand mould has been simulated. Unsteady heat conduction eq. in two-dimensional form governs the physical problem. Convective boundary conditions have been considered at the interface where molten metal meets the mould cavity surface. Heat conduction eq. in unsteady state and transient state have been solved by using Two dimensional finite analyses difference method using MATLAB to study thermal flow and cooling rate. The properties of materials utilized are green sand and pure Al, Al6063 and brass. The results obtained are: cooling rate of pure Aluminum, Al6063 and brass in green sand mould for 2D casting for unsteady problem and temperature distribution in steady case.

Keywords: Explicit scheme; Casting solidification; simulation

1. Introduction

Casting which additionally referred to a role as founding is one of the soonest metal forming systems known not being. It for the most part means the pouring of molten metal into the refractory mould with an enclosure of the shape to be made then permitting it to solidify. At the point when hardened, article is taken out from the refractory mould either by breaking the mould or ejecting the mould part. The solidified part is called casting. Casting has been lengthily utilized in manufacturing because of its many applications and advantages. Tools required for casting mould are very simple and cheap and any intricate shape, either external or internal can be casted that would be otherwise challenging or uneconomical to make by other methods. A large variety of materials are used in foundries for manufacturing mould and cores. The most commonly used materials are metals or other cold setting materials that can be made after mixing of two or more components together like: epoxy, concrete, plaster and clay.

The reasoning is difficult to follow, but Field is also arrived at a parabolic relationship between thickness solidification and time. Although much simpler, analytically, the heat flow problem in the sand casting have only been considered separately by Chvorinov [1]. Chvorinov simplifies the problem by neglecting any temperature gradients in the casting and concludes that time for complete freezing should be proportional to,

$$\left(\frac{\text{Casting Volume}}{\text{Casting Surface Area}} \right)^2$$

* Corresponding Author

Choudhari *et. al.*, [2] conducted Modelling and Simulation with Experimental Validation of Temperature Distribution during Solidification Process in Sand Casting. They studied heat flow within the casting, as well as from the casting to the mould, and finally acquire the temperature history of all points inside the casting. They found that that most important instant of time is when the hottest region inside the cavity of casting is solidifying. They performed Transient thermal analysis using ANSYS software to obtain the temperature distribution in the casting process. They obtained results by simulation software and compared that with the experimental reading of temperature. They also studied the significance of filling pattern and appropriate orientation of gating system. In the end they concluded that the simulation of casting process helps in finding temperature distribution of different parts of the mould. They also concluded that simulation helps in reducing the cost of development and material utilization (yield).

A. Venkatesan [3] in his study established, a system for FE modelling of solidification of casting. The striking elements of the system are: incorporation of latent heat through enthalpy strategy, integration of air gap by coincident node process, capacity. They wrote a on C++ language utilizing Gaussian elimination approach to explain the matrices. Utilizing this program, solidification of infinite section of water was simulated and the outcomes were compared with reported literature and ANSYS and were discovered to be in great agreement. Likewise, solidification of Al-6 wt. % Si alloys was simulated and linked with experimental results and ANSYS. Time acquired from the present work was 1200 s with that of literature 1100 s and ANSYS of 900 s. So it was discovered to be in great agreement with the examination and trial discoveries. The program was constrained to 2D heat exchange analysis utilizing linear quadrilateral components. The program could be extended for anticipating the grain structure. From the results, the solid-liquid interface speed (R) and cementing rate (dT/dt) could be figured and utilizing these thermal gradients (G) could be discovered and there by the most plausible grain structure could be predicted.

Choudhari *et. al.*, [4] studied Optimum Design and Analysis of Riser for Sand Casting using ANSYS. They find that simulation of the solidification process allows visualization of solidification inside a casting and helps in finding last freezing regions or hot spots. They noticed that simulation also helps in optimizing the placement and design of feeders and feeding aid. They concluded that solidification defect can be minimized after finding optimum location of riser. They determined that simulation can help in optimizing dimensions of riser and casting feeding efficiency. They also validated their results of optimized riser dimensions based on simulation by carrying out actual trials in a foundry. In the end they concluded that utilizing sleeve as a feed aid helps in reducing riser dimensions from 60 mm to 50mm which helps in increasing the casting yield.

Hassan Jafari *et. al.*, [5] completed computer helped thermal investigation to exactly measure the thermal attributes of AZ91D magnesium composite granules amid in situ liquefying and hardening in investment casting procedure. Ceramic shell moulds of two distinct thicknesses outfitted with profoundly touchy thermocouples at three unique areas were arranged to give a scope of heating and cooling rates amid in situ liquefying and cementing. The outcomes uncovered that different heat regimes were experienced by the granules at distinctive areas of the mould amid heating, which led to asynchronous melting of the granules. It was found that both dissolving beginning and finishing were expanded with expanding heating rate; conversely inverse performance was seen amid cooling. The onset and the end of hardening temperatures and duration diminished with expanding cooling and solidification rates. The data from this methodology is extremely pivotal for suppressing mould-metal response particularly amid cooling in casting of magnesium alloys by investment casting procedure.

Vijayaram *et. al.*, [6] in their paper, talks about the significance of heat transfer in the simulation procedure. Their paper surveys the points of interest of computer modelling of solidification of castings in metallurgical designing foundries. Since, computers turned

out to be broadly accessible in industry, analysts have been chipping away at the advancement of projects to recreate the hardening of castings.

Masoud Jabbari and Azin Hosseinzadeh [7] Numerical modelling of coupled heat transfer and phase transformation for solidification of the gray cast iron. The nucleation and growth hypothesis was utilized, and cooling rate was executed as a key consider in the solidification stages. A FDM model was developed for measure of graphite, cementite, and aggregate austenite on the premise of the cooling rate and level principle. As the cooling rate builds, the unstable stages increment. It is found that expanding cooling rate brings about the increment of cementite stage and the abatement of graphite and austenite stages. Hardness of gray cast iron reductions as the volume portion of graphite goes up. Increasing the cementite, results in the improvements of the hardness of the gray cast iron. The proposed equations developed by numerical modelling find in decent concurrence with the experiments results. The present work is to enquire the conduction heat transfer in a sand mould employing finite difference scheme. This study examines unsteady cooling conduction heat transfer through the solidification of an Al 6061 casting in green sand mould. Governing eq. has been solved using MATLAB R2012a.

2. Mathematical Formulation

2.1. Physical Domain

Figure 1 demonstrates the schematic of the rectangular mould cavity. Solid part is the casting to be made where molten metal is poured while outside portion is of green sand mould. Liquid metal is poured in the mould cavity from the top opening. Thick lines which represent the casting walls on which convective boundary condition have been considered, which means that heat transferred by conduction is equal to the heat transferred by convection. Heat is exchanged to the surroundings via walls of the mould cavity.

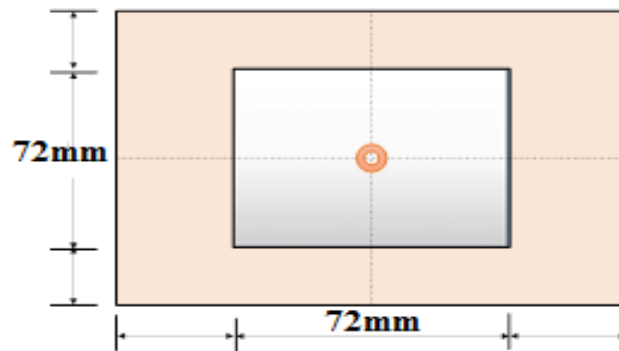


Figure 1. Schematic of Mould Cavity

2.2. Governing Equations

$$\rho C_p \frac{\partial T}{\partial t} + \left(u \frac{\partial T}{\partial x} + v \frac{\partial T}{\partial y} \right) = k \left(\frac{\partial^2 T}{\partial x^2} + \frac{\partial^2 T}{\partial y^2} \right) \quad (1)$$

Above mathematical statement is two-dimensional Energy eq.. First term on the left hand side of the eq. characterizes the variation of the temperature with the time which represents the unsteady heat transfer and second term is convective part which comes into play due to movement of the molecules, while term on right hand side characterizes the variation in the spatial direction which represents the diffusive part. Other two modes of

heat transfer, convection and radiation have been neglected inside the cavity. So the above eq. will reduce to a simple form by neglecting the second term on the left hand side,

$$\rho C_p \frac{\partial T}{\partial t} = k \left(\frac{\partial^2 T}{\partial x^2} + \frac{\partial^2 T}{\partial y^2} \right) \quad (2)$$

A simplified form of the above governing eq. can also be written as

$$\frac{\partial T}{\partial t} = \alpha \left(\frac{\partial^2 T}{\partial x^2} + \frac{\partial^2 T}{\partial y^2} \right) \quad (3)$$

Where: $\alpha = k/\rho C_p$ is thermal diffusivity in m^2/s , k is thermal conductivity in W/m-K, ρ is density in Kg/m^3 , C_p is specific heat KJ/Kg-K, T is temperature in Kelvin (K), t is time in seconds. Table 1 represents the thermo physical properties of all the materials.

The above mathematical statement is in the form of partial differential eq. (PDE), to get an answer it must be communicated in the form of estimated solution so that a computer which can perform just math and legitimate operations can be worked to obtain a solution. Taylor series expansion will be considered to change these partial derivative terms in mathematical structure which can be expressed as,

Table 1. Thermo Physical Properties of Molten Metal and Sand

Properties	Al6063	Pure Al	Brass	Sand
Specific heat (KJ/Kg-K)	0.9	0.8963	0.377	1172.3
Density (Kg/m^3)	2700	2690	8525	1494.71
Thermal conductivity (W/m-K)	201	237	115	0.52
Melting Point (K)	928	973	900	

X-direction

$$T(x + \Delta x, y) = T(x, y) + \frac{\partial T(x, y)}{\partial x} \frac{\Delta x}{1!} + \frac{\partial^2 T(x, y)}{\partial x^2} \frac{(\Delta x)^2}{2!} + \frac{\partial^3 T(x, y)}{\partial x^3} \frac{(\Delta x)^3}{3!} + O(\Delta x)^4 \quad (4)$$

$$T(x - \Delta x, y) = T(x, y) - \frac{\partial T(x, y)}{\partial x} \frac{\Delta x}{1!} + \frac{\partial^2 T(x, y)}{\partial x^2} \frac{(\Delta x)^2}{2!} - \frac{\partial^3 T(x, y)}{\partial x^3} \frac{(\Delta x)^3}{3!} + O(\Delta x)^4 \quad (5)$$

Likewise in y-direction

$$T(x, y + \Delta y) = T(x, y) + \frac{\partial T(x, y)}{\partial y} \frac{\Delta y}{1!} + \frac{\partial^2 T(x, y)}{\partial y^2} \frac{(\Delta y)^2}{2!} + \frac{\partial^3 T(x, y)}{\partial y^3} \frac{(\Delta y)^3}{3!} + O(\Delta y)^4 \quad (6)$$

$$T(x, y - \Delta y) = T(x, y) - \frac{\partial T(x, y)}{\partial y} \frac{\Delta y}{1!} + \frac{\partial^2 T(x, y)}{\partial y^2} \frac{(\Delta y)^2}{2!} - \frac{\partial^3 T(x, y)}{\partial y^3} \frac{(\Delta y)^3}{3!} + O(\Delta y)^4 \quad (7)$$

Eq. 4 and 5 are Taylor series expansion in x-direction for forward and backward respectively while eq. 6 and 7 are for y-direction.

Present governing eq. involves both first and second order partial derivative term first we will find the second order spatial terms of the heat conduction eq. $\frac{\partial^2 T}{\partial x^2}$ and $\frac{\partial^2 T}{\partial y^2}$,

Including the mathematical statement 4 and 5 and in the wake of doing some math operation we will at last get,

$$\frac{\partial^2 T}{\partial x^2} = \frac{T(x+\Delta x, y) + T(x-\Delta x, y) - 2T(x, y)}{(\Delta x)^2} + O(\Delta x)^2 \quad (8)$$

Similarly for second order partial term in y-direction

$$\frac{\partial^2 T}{\partial y^2} = \frac{T(x,y+\Delta x)+T(x,y-\Delta x)-2T(x,y)}{(\Delta y)^2} + O(\Delta y)^2 \quad (9)$$

Above constructions are called central differencing scheme for second order partial derivative term, where $O(\Delta x)^2$ and $O(\Delta y)^2$ represents that the formulation is second order accurate.

Graphical representation of the above eq. is indicated in Figure 2 Element demonstrated in figure, denotes a collocated grid where ϕ can be any dependent parameter. Element in left hand side Figure (a) is in Cartesian structure while element in right hand side Figure (b) is in vector structure. It is a five-node element formulation, where $\phi(i, j)$ characterizes the central node while every single other node have been spoken to comparing to this.

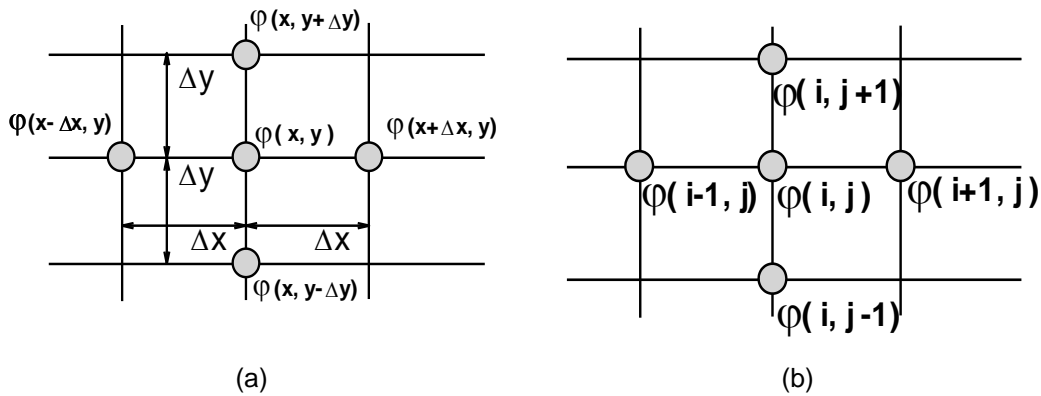


Figure 2. Grid element Layout

Temporal derivative term is first order partial term and can be discretized either by explicit scheme or by implicit scheme,

$$\frac{T_{i,j}^{n+1}-T_{i,j}^n}{\Delta t} = \alpha \left(\frac{T_{i+1,j}^n+T_{i-1,j}^n-2T_{i,j}^n}{(\Delta x)^2} + \frac{T_{i,j+1}^n+T_{i,j-1}^n-2T_{i,j}^n}{(\Delta y)^2} \right) \quad (10)$$

$$\frac{T_{i,j}^{n+1}-T_{i,j}^n}{\Delta t} = \alpha \left(\frac{T_{i+1,j}^{n+1}+T_{i-1,j}^{n+1}-2T_{i,j}^{n+1}}{(\Delta x)^2} + \frac{T_{i,j+1}^{n+1}+T_{i,j-1}^{n+1}-2T_{i,j}^{n+1}}{(\Delta y)^2} \right) \quad (11)$$

Eq. 10 and 11 represents the explicit and implicit discretization of eq. 3. In explicit scheme only one term is at the next time level (n+1) which is an unknown quantity while every single other terms are at same time level (n) which are known. In implicit scheme spatial derivative terms are also at the next time level (n+1) which makes it hard to handle in PC code. Explicit scheme is easy to code yet obliges a condition to fulfill which is known as stability condition presented in eq. 12 and leaves a cut-off on the time step for a particular grid chosen while in implicit scheme stability condition does not applied.

$$\alpha \times dt \left(\frac{1}{(\Delta x)^2} + \frac{1}{(\Delta y)^2} \right) \leq \frac{1}{2} \quad (12)$$

In present work explicit scheme has been selected because of straightforwardness of the scheme, we know that value at time 'n+1' is unknown while values at time 'n' are known. So from above eq. it can be noted that all the terms on right hand side are at time 'n' (known) while stand out term at time 'n+1' is there in left hand side which can be effectively figured as,

$$T_{i,j}^{n+1} = T_{i,j}^n + \alpha \Delta t \left(\frac{T_{i+1,j}^n+T_{i-1,j}^n-2T_{i,j}^n}{(\Delta x)^2} + \frac{T_{i,j+1}^n+T_{i,j-1}^n-2T_{i,j}^n}{(\Delta y)^2} \right) \quad (13)$$

2.3. Boundary Conditions

$$\begin{aligned} \text{At } x = 0 & \quad q = k \frac{\partial T}{\partial x} = h_f(T - T_\infty) \\ \text{At } x = L & \quad q = k \frac{\partial T}{\partial x} = -h_f(T - T_\infty) \\ \text{At } y = 0 & \quad q = k \frac{\partial T}{\partial y} = h_f(T - T_\infty) \\ \text{At } y = H & \quad q = k \frac{\partial T}{\partial y} = -h_f(T - T_\infty) \end{aligned}$$

Where q = heat transfer in Joules (J), h_f = latent heat of fusion in (KJ/Kg) and T_∞ = Ambient temperature in Kelvin (K)

3. Result and Discussion

A grid size of 72×72 is sufficiently reasonable to portray the flow and heat transfer of the procedure. Time step has been kept equal to $dt = 0.0001$ to justify the stability condition:

$$\alpha \times dt \left(\frac{1}{(dx)^2} + \frac{1}{(dy)^2} \right) \leq \frac{1}{2}$$

All three phenomenons of heat transfer conduction, convection and radiation will contribute toward the solution of this problem (solidification of molten metal in green sand mould. But conduction will dominate over convection and radiation which has been considered in the present study.

Figure 3 (a-c) represents the cooling rate of the pure aluminum, Al 6063 and brass in the green sand. Melting point temperature of these three materials are 971K, 928K and 900K respectively for pure aluminum, Al 6063 and brass. Central point temperature of the mould cavity has been plotted. At melting point temperature liquid metal is poured into the mould cavity which is initial foundry shop temperature. Temperature on the walls of the cavity is atmospheric temperature and is equal 310K. One can notice that from the figure that when time step dt is equal to '0.001' temperature is around melting point temperature and as the time increases, temperature starts to cool down and reaches to atmospheric temperature after large number of iteration. We can conclude from the cooling curve that the time required for cooling from melting point temperature to atmospheric temperature it more in Al6063 than brass and pure aluminum casting and the cooling time for brass casting is more than pure aluminum.

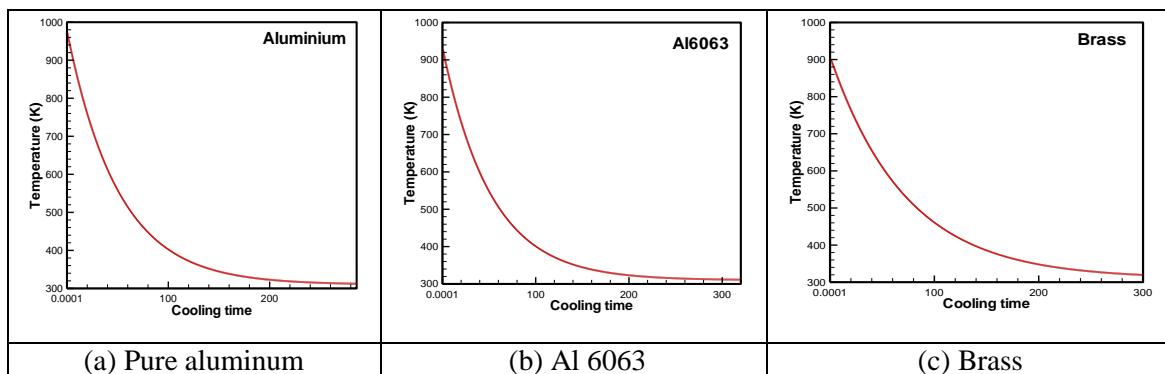


Figure 3. Cooling Curve in Casting

Figure 4 (a-c) represents the temperature distribution of all the three materials Al 6063, Brass and pure aluminum respectively for casting in green sand mould for steady state

condition. This temperature distribution has been plotted on a grid size of 72×72 . This surf has been plotted in full part of the mould cavity. One can notice that the maximum temperature is at the center of the cavity at which molten metal poured. Al 6063 is poured at (928K), Brass at (900K) and pure aluminum at (973K), then it decreases towards the walls of the cavity in both x-direction and y-direction respectively, which are at atmospheric temperature (310K).

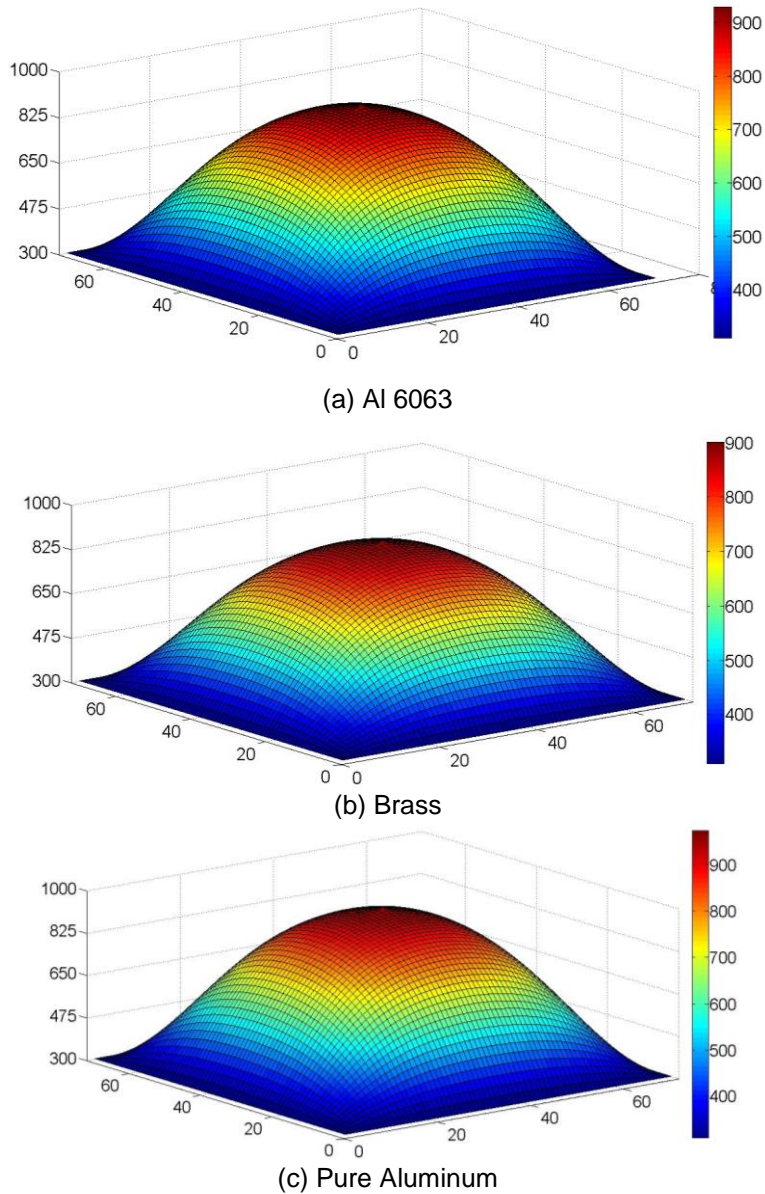


Figure 4. Temperature Distribution in Casting and Sand Mould during Solidification (Steady State)

References

- [1] N. G. Chvorinov, "Control of the solidification of casting by calculation", vol. 27, (1940), pp. 177, 201, 222.
- [2] C. M. Choudhary, B. E. Narkhede and S. K. Mahajan, "Modelling and Simulation with Experimental Validation of Temperature Distribution during Solidification Process in Sand Casting", International Journal of Computer Applications, vol. 78, (2013), pp. 23-29.

- [3] A. Venkatesan, V. M. Gopinath and A. Rajadurai, "Simulation of casting solidification and its grain structure prediction using FEM", *Journal of Materials Processing Technology*, vol. 168, (2005), pp. 10-15.
- [4] C. M. Choudhari, K. J. Padalkar, K. K. Dhumal, B. E. Narkhede and S. K. Mahajan, "Defect free casting by using simulation software", *Applied Mechanics and Materials*, vol. 313-314, (2013), pp. 1130-1134.
- [5] H. Jafari, M. H. Idris, A. Ourdjini and S. Farahany, "In situ melting and solidification assessment of AZ91D granules by computer-aided thermal analysis during investment casting Process", *Materials and Design*, vol. 50, (2013), pp. 181-190.
- [6] T. R. Vijayaram, S. Sulaiman, A. M. S. Hamouda and M. H. M. Ahmad, "Numerical Simulation of Casting Solidification in Permanent Metallic Molds", *Journal of Materials Processing Technology*, vol. 178, (2006), pp. 29-33.
- [7] M. Jabbari and A. Hosseinzadeh, "Numerical modelling of coupled heat transfer and phase transformation for solidification of the gray cast iron", *Computational Materials Science*, vol. 68, (2013), pp. 160-165.